

Research Article

Reduced-Order Antisynchronization of Chaotic Systems via Adaptive Sliding Mode Control

Wafaa Jawaada,¹ M. S. M. Noorani,¹ M. Mossa Al-Sawalha,² and M. Abdul Majid²

¹ School of Mathematical Sciences, Universiti Kebangsaan Malaysia, 43600 Bangi, Selangor, Malaysia

² Mathematics Department, Faculty of Science, University of Hail, Hail 81451, Saudi Arabia

Correspondence should be addressed to M. Mossa Al-Sawalha; sawalha_moh@yahoo.com

Received 10 May 2013; Accepted 26 August 2013

Academic Editor: Juan Carlos Cortés López

Copyright © 2013 Wafaa Jawaada et al. This is an open access article distributed under the Creative Commons Attribution License, which permits unrestricted use, distribution, and reproduction in any medium, provided the original work is properly cited.

A novel reduced-order adaptive sliding mode controller is developed and experimented in this paper to antisynchronize two different chaotic systems with different order. Based upon the parameters modulation and the adaptive sliding mode control techniques, we show that dynamical evolution of third-order chaotic system can be antisynchronized with the projection of a fourth-order chaotic system even though their parameters are unknown. The techniques are successfully applied to two examples: firstly Lorenz (4th-order) and Lorenz (3rd-order) and secondly the hyperchaotic Lü (4th-order) and Chen (3rd-order). Theoretical analysis and numerical simulations are shown to verify the results.

1. Introduction

Nonlinearity is ubiquitous in the natural world around us such as in chemical reactions, cardiac arrhythmias, brain neural waves, relativity, population growth rates, and atmospheric changes. The study of the chaotic nature of the nonlinear dynamical systems, although complex and challenging, paves a way to understand the laws of nature. An understanding of the disorder and oscillating nature of these systems and their instability leads to many useful real-world science and engineering applications. Until some decades, the only systems that could be understood were those that were believed to be linear or systems that follow predictable patterns and arrangements. However, the advent of high-speed computers has provided mathematicians some considerable accessibility in the analysis of nonlinear systems and the chaos theory is one of the many milestones. Lately, the theory of chaos has become one of the most noteworthy and undoubtedly valuable subjects of research due to its wide and numerous applications. There is a need to understand and to have a reasonable control over the unforeseen natural events and phenomena. “A very small cause which escapes our notice determines a considerable effect that we cannot fail to see...even if the case that the natural laws had no

longer secret for us...we could only know the initial situation approximately...It may happen that small differences in initial conditions produce very great ones in the final phenomena.” [1–4].

The work of Pecora and Carroll [5] on synchronization of chaotic systems has immensely influenced the modern research. This research has led to the development of a wide range of approaches in the understanding of not only the synchronization but also the antisynchronization of chaotic dynamical systems [6–14].

Antisynchronization (AS) or antiphase synchronization (APS), an extended scope of synchronization, is a phenomenon that the state vectors of the synchronized systems have the same amplitude but opposite signs as those of the driving system. There are many methods discussed in the literature on the synchronization and antisynchronization of dynamical systems of equal and unequal orders. Synchronization of a slave system with projections of a master system is dealt with in the reduced-order synchronization. However, it is important to make a distinction here that the problem of the reduced-order synchronization differs from the partial synchronization where the latter is mainly for coupling of two chaotic systems which have an equal order. The main characteristic feature of the reduced-order synchronization

is that the order of the slave system is less than the master system.

In this paper, we address the reduced-order antisynchronization of chaotic systems via adaptive sliding mode controller. A great deal of research has already been undertaken mainly on the synchronization and the antisynchronization between two chaotic systems with the same order. However, due to the complex nature of the chaotic dynamical systems, a thorough understanding of the antisynchronization between two chaotic systems of unequal order is vital as they have much wider applications. This gave us the motivation to introduce this work.

2. Problem Formulation

Consider a chaotic system described by the following nonlinear differential equation:

$$\dot{x} = f(x) + F(x)\alpha, \quad (1)$$

where $x \in R^n$ is the state vector, $\alpha \in R^p$ is the unknown parameter vector of the system, $f(x)$ is an $n \times 1$ matrix, $F(x)$ is an $n \times p$ matrix, and the elements $F_{ij}(x)$ in matrix $F(x)$ satisfy $F_{ij}(x) \in L_\infty$. Equation (1) is assumed to be the master (drive) system, and now we define the slave (response) system as follows:

$$\dot{y} = g(y) + G(y)\beta + u(t), \quad (2)$$

where $y \in R^m$ is the state vector, $\beta \in R^q$ is the unknown parameter vector of the system, $g(y)$ is an $m \times 1$ matrix, $G(y)$ is an $m \times q$ matrix and the elements $G_{ij}(y)$ in matrix $G(y)$ satisfy $G_{ij}(y) \in L_\infty$, and $u(t) \in R^m$ is the controller to be designed such that it antisynchronizes the states of the master and slave systems.

We assume that systems (1) and (2) satisfy the condition $m < n$; that is, the order of the slave system is lower than that of the master system. With this condition, we can only attain the antisynchronization in reduced-order that is controlling a slave system to be the projection of the master system. To this end, we break the master system into two parts as follows:

$$\dot{x}_1 = f_1(x) + F_1(x)\alpha, \quad (3)$$

where $x_1 \in R^m$, $f_1 : R^n \rightarrow R^m$, and $F_1 : R^n \rightarrow R^{m \times p}$, the rest of the projections, can be denoted as

$$\dot{\bar{x}}_1 = \bar{f}_1(x) + \bar{F}_1(x)\alpha, \quad (4)$$

where $\bar{x}_1 \in R^l$, $\bar{f}_1 : R^n \rightarrow R^l$, and $\bar{F}_1 : R^n \rightarrow R^{l \times p}$ where $m + l = n$; errors can be expressed as

$$\dot{e} = f_1(x) + F_1(x)\alpha + g(y) + G(y)\beta + u(t), \quad (5)$$

where $e = y + x_1$.

To gain reduced order antisynchronization between the master and slave system is to basically design the controller $u(t) \in R^m$ such that

$$\lim_{t \rightarrow \infty} \|e\| = \lim_{t \rightarrow \infty} \|y(t, y_0) + x(t, (x_1)_0)\| = 0, \quad (6)$$

where $\|\cdot\|$ is the Euclidean norm.

The sliding mode control method of antisynchronization involves two major stages: (1) choosing a suitable switching surface for the desired sliding motion and (2) designing the sliding mode controller that brings any orbit in phase space to the switching surface and then achieves the antisynchronization of the chaotic systems even in the presence of parameter and disturbance uncertainties. This is precisely why this method of antisynchronization is considered to be robust under uncertainties and external disturbances.

2.1. Sliding Surface Design. The sliding surface can be defined as follows:

$$s(e) = Ce, \quad (7)$$

where $C = [c_1, c_2, c_3]$ is a constant vector. The equivalent control approach is found by the fact that $\dot{s}(e) = 0$ is a necessary condition for the state trajectory to stay on the switching surface $s(e) = 0$. Hence, when in sliding mode, the controlled system satisfies the following conditions:

$$\begin{aligned} s(e) &= 0, \\ \dot{s}(e) &= 0. \end{aligned} \quad (8)$$

2.2. Design of the Sliding Mode Controller. In what follows, the appropriate sliding mode controller will be designed according to the sliding mode control theory. Choosing the controller $u(t)$

$$u(t) = -f_1(x) - g(y) - F_1(x)\hat{\alpha} - G(y)\hat{\beta} - Kw(t), \quad (9)$$

where $K = [k_1, k_2, k_3]^T$ is a constant positive gain vector and $w(t) \in R$ is the control input that satisfies:

$$w(t) = \begin{cases} w^+(t) & s(e) \geq 0, \\ w^-(t) & s(e) < 0 \end{cases} \quad (10)$$

and $s = s(e)$ is a switching surface which prescribes the desired dynamics. And $\hat{\alpha}$ and $\hat{\beta}$ are the parameter estimates of α and β , respectively. The control input can be determined as:

$$w(t) = \left[\frac{s}{|s| + \gamma} \right], \quad (11)$$

where γ is a positive real number. The resultant error dynamics is then

$$\dot{e} = F_1(x)(\alpha - \hat{\alpha}) + G(y)(\beta - \hat{\beta}) - K \left[\frac{s}{|s| + \gamma} \right]. \quad (12)$$

The parameters update laws can be chosen as

$$\begin{aligned} \dot{\hat{\alpha}} &= F_1(x)^T \lambda, & \hat{\alpha}(0) &= \hat{\alpha}_0, \\ \dot{\hat{\beta}} &= G(y)^T \lambda, & \hat{\beta}(0) &= \hat{\beta}_0, \end{aligned} \quad (13)$$

where $\lambda = s[c_1, c_2, c_3]^T = sC^T$ and $\hat{\alpha}_0$ and $\hat{\beta}_0$ are the initial values of the update parameters $\hat{\alpha}$ and $\hat{\beta}$, respectively.

2.3. Stability Analysis. The following theorem contains the necessary conditions for the stability of error system in (12).

Theorem 1. *Considering that adaptive sliding mode control input law in (9) is used to control error system in (5) with update laws of parameters in (13), then error system in (12) is asymptotically stable.*

Proof. To check the stability of the controlled system, one can consider the following Lyapunov candidate function:

$$V = \frac{1}{2}s^2 + \frac{1}{2}\|\alpha - \hat{\alpha}\|^2 + \frac{1}{2}\|\beta - \hat{\beta}\|^2. \quad (14)$$

The time derivative of (14) is

$$\begin{aligned} \dot{V} &= \dot{s}s - (\alpha - \hat{\alpha})^T \dot{\hat{\alpha}} - (\beta - \hat{\beta})^T \dot{\hat{\beta}} \\ &= sC\dot{e} - (\alpha - \hat{\alpha})^T \dot{\hat{\alpha}} - (\beta - \hat{\beta})^T \dot{\hat{\beta}} \\ &= s\dot{e}^T C^T - (\alpha - \hat{\alpha})^T \dot{\hat{\alpha}} - (\beta - \hat{\beta})^T \dot{\hat{\beta}}. \end{aligned} \quad (15)$$

Introducing update laws in (13) into the right side of (15), one obtains

$$\begin{aligned} \dot{V} &= \left[(\alpha - \hat{\alpha})^T F(x)^T + (\beta - \hat{\beta})^T G(y)^T - K^T \left[\frac{s}{|s| + \gamma} \right] \right] sC^T \\ &\quad - (\alpha - \hat{\alpha})^T F(x)^T \lambda - (\beta - \hat{\beta})^T G(y)^T \lambda \\ &= (\alpha - \hat{\alpha})^T F(x)^T \lambda + (\beta - \hat{\beta})^T G(y)^T \lambda - K^T C^T \left[\frac{s^2}{|s| + \gamma} \right] \\ &\quad - (\alpha - \hat{\alpha})^T F(x)^T \lambda - (\beta - \hat{\beta})^T G(y)^T \lambda. \end{aligned} \quad (16)$$

Then (16) reduces to

$$\dot{V} = -CK \left[\frac{s^2}{|s| + \gamma} \right]. \quad (17)$$

Since both $s^2 > 0$ and $|s| > 0$ when $e \neq 0$ and $CK > 0$, the inequality $\dot{V} < 0$ holds.

Since V is positive definite and \dot{V} is negative semidefinite, then the error system is stable in the sense of Lyapunov and the slave system (1) antisynchronizes the master system (2) asymptotically and globally. This completes the proof. \square

3. Systems Description

The hyperchaotic Lorenz system [15] is written as

$$\begin{aligned} \dot{x} &= a(y - x) + w, \\ \dot{y} &= bx - xz - y, \\ \dot{z} &= xy - cz, \\ \dot{w} &= xz + rw, \end{aligned} \quad (18)$$

where x, y, z , and w are state variables and a, b, c , and r are the system unknown parameters. When $a = 36, b = 20, c = 8/3$, and $r = 1.3$, system (18) has hyperchaotic attractor. The projections of the hyperchaotic Lorenz system attractor are shown in Figure 1. The three-dimensional Lorenz system [16] is given by

$$\begin{aligned} \dot{x} &= a(y - x), \\ \dot{y} &= bx - xz - y, \\ \dot{z} &= xy - cz, \end{aligned} \quad (19)$$

where x, y , and z are, respectively, proportional to the convective velocity, the temperature difference between descending and ascending flows, and the mean convective heat flows. Also, a, b , and the so-called bifurcation parameter c are real constants. Throughout this paper, we set $a = 10, b = 28$, and $c = 8/3$ such that the system exhibits chaotic behavior. The chaotic attractor is shown in Figure 2. The hyperchaotic Lü system [17] is described by

$$\begin{aligned} \dot{x} &= a(y - x) + w, \\ \dot{y} &= -xz + by, \\ \dot{z} &= xy - cz, \\ \dot{w} &= xz + rw, \end{aligned} \quad (20)$$

where x, y, z , and w are state variables and a, b, c , and r are real constants. When $a = 36, b = 20$, and $c = 3, -1.03 \leq r \leq -0.46$, system (20) has periodic orbit; when $a = 36, b = 3, c = 20$, and $-0.46 < r \leq -0.35$, system (20) has chaotic attractor, when $a = 36, b = 3, c = 20$, and $-0.35 < r \leq 1.3$, system (20) has hyperchaotic attractor. The projections of the hyperchaotic Lü system system attractor are shown in Figure 3. The three-dimensional Chen system [18] is given by

$$\begin{aligned} \dot{x} &= a(y - x), \\ \dot{y} &= (b - a)x - xz + by, \\ \dot{z} &= xy - cz, \end{aligned} \quad (21)$$

where x, y , and z are state variables and a, b , and c are positive parameters. Bifurcation studies show that, with the parameters $a = 35$ and $b = 28$, system (21) exhibits chaotic behavior when $c = 3$. The chaotic attractor is shown in Figure 4.

In order to observe reduced order antisynchronization behavior between chaotic systems via adaptive sliding mode control, we consider two examples. The first one is hyperchaotic Lorenz system in (18) as a master system with three-dimensional Lorenz system in (19) as the slave system. The second example is hyperchaotic Lü system (20) as a master system with three-dimensional Chen system which is described in (21) as the slave system.

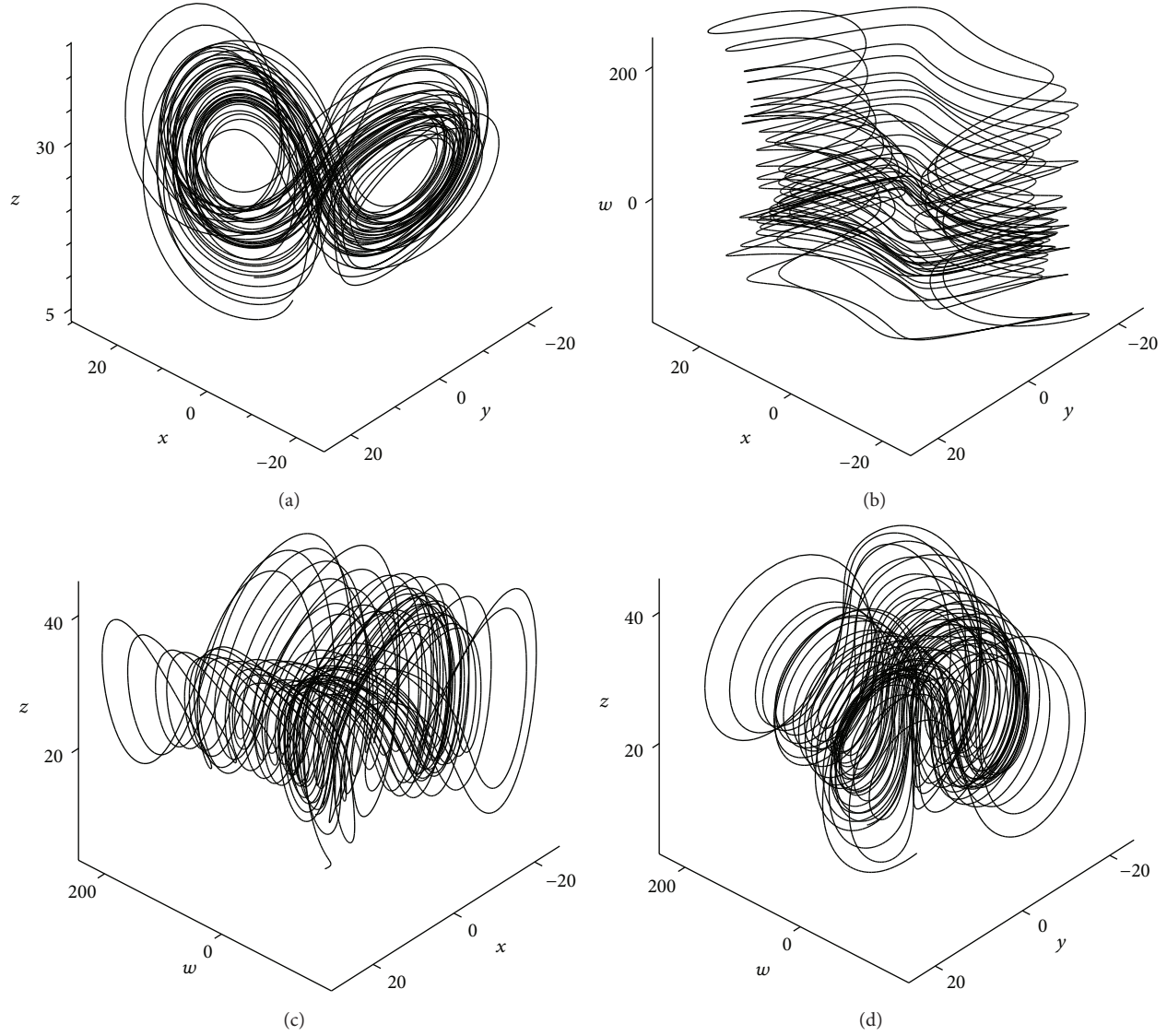


FIGURE 1: Typical dynamical behavior of hyperchaotic Lorenz system. (a) Projection in (x, y, z) space; (b) projection in (w, x, y) space; (c) projection in (x, w, z) space; (d) projection in (w, y, z) space.

4. Adaptive Reduced-Order Sliding Mode Antisynchronization between Hyperchaotic Lorenz System and the Three-Dimensional Lorenz System

For the hyperchaotic Lorenz system, the master system is considered to be the projections in the direction of x , y , and z only. So it can be written as follows:

$$\begin{aligned}\dot{x}_1 &= a_1(y_1 - x_1) + w_1, \\ \dot{y}_1 &= b_1x_1 - x_1z_1 - y_1, \\ \dot{z}_1 &= x_1y_1 - c_1z_1\end{aligned}\quad (22)$$

and the slave system can be written as

$$\dot{x}_2 = a_2(y_2 - x_2) + u_1,$$

$$\dot{y}_2 = b_2x_2 - x_2z_2 - y_2 + u_2,$$

$$\dot{z}_2 = x_2y_2 - c_2z_2 + u_3,$$

(23)

where u_1 , u_2 , and u_3 are three control functions to be designed.

The error dynamics is represented by

$$\dot{e}_1 = a_1(y_1 - x_1) + a_2(y_2 - x_2) + w_1 + u_1,$$

$$\dot{e}_2 = b_1x_1 - x_1z_1 - y_1 + b_2x_2 - x_2z_2 - y_2 + u_2,$$

$$\dot{e}_3 = x_1y_1 - c_1z_1 + x_2y_2 - c_2z_2 + u_3,$$

(24)

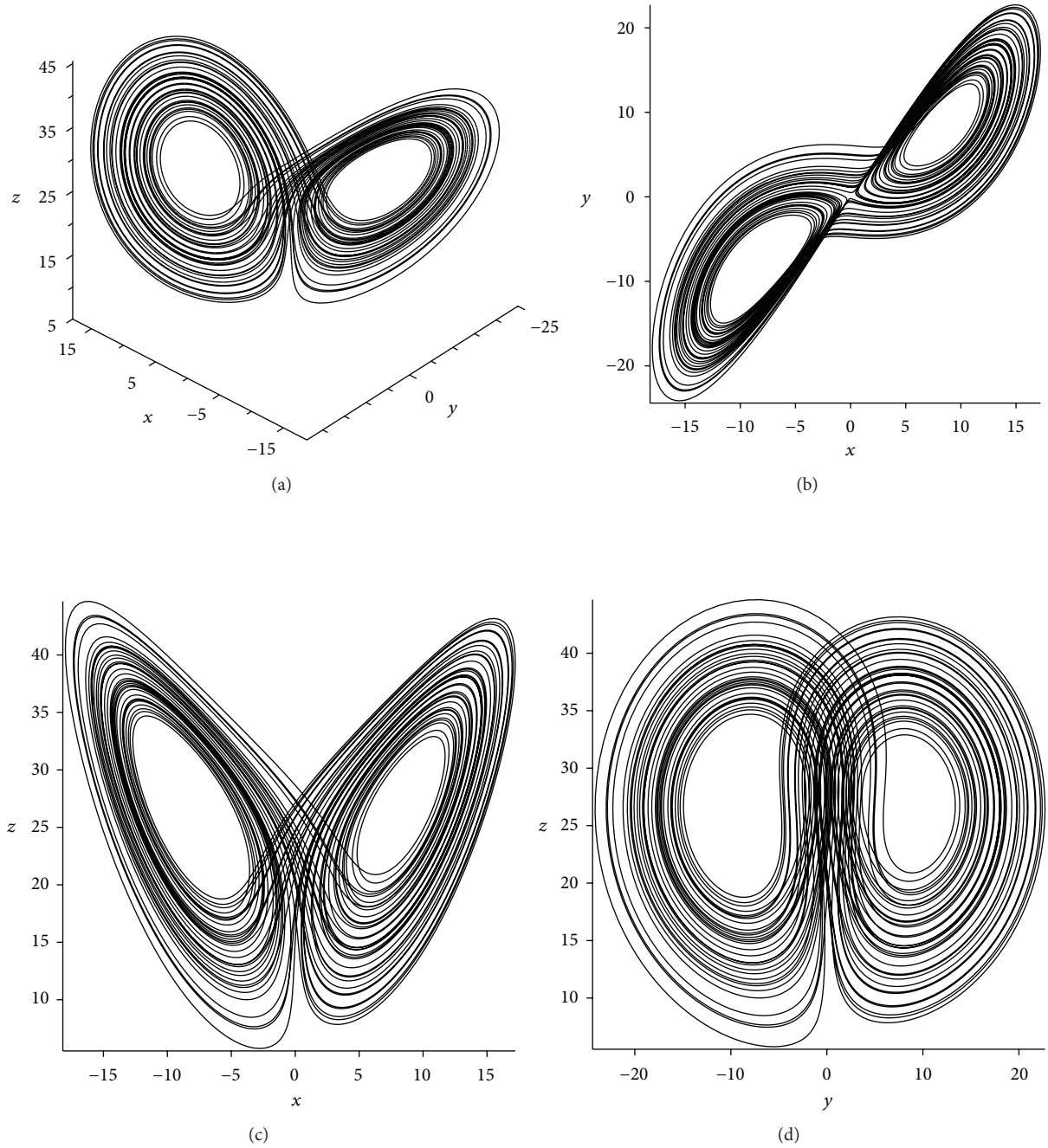


FIGURE 2: Typical dynamical behavior of three-dimensional Lorenz system. (a) Projection in (x, y, z) space; (b) projection in (x, y) space; (c) projection in (x, z) space; (d) projection in (y, z) space.

where $e_1 = x_1 + x_2$, $e_2 = y_1 + y_2$, and $e_3 = z_1 + z_2$. The control parameters are chosen as $C = (-1, 1, 1)$, $K = (0, 6, 0)^T$ and $\gamma = 0.01$. Then the switching surface is equal to

$$\begin{aligned} s(e) &= -e_1 + e_2 + e_3, \\ w(t) &= \frac{s}{|s| + 0.01}, \end{aligned} \quad (25)$$

and then the adaptive sliding mode control law for the system in (24) is

$$\begin{aligned} u_1 &= -\hat{a}_1(y_1 - x_1) - \hat{a}_2(y_2 - x_2) - w_1, \\ u_2 &= -\hat{b}_1 x_1 + x_1 z_1 + x_2 z_2 - \hat{b}_2 x_2 + e_2 - \frac{6s}{|s| + 0.01}, \\ u_3 &= -x_1 y_1 + \hat{c}_1 z_1 - x_2 y_2 + \hat{c}_2 z_2, \end{aligned} \quad (26)$$

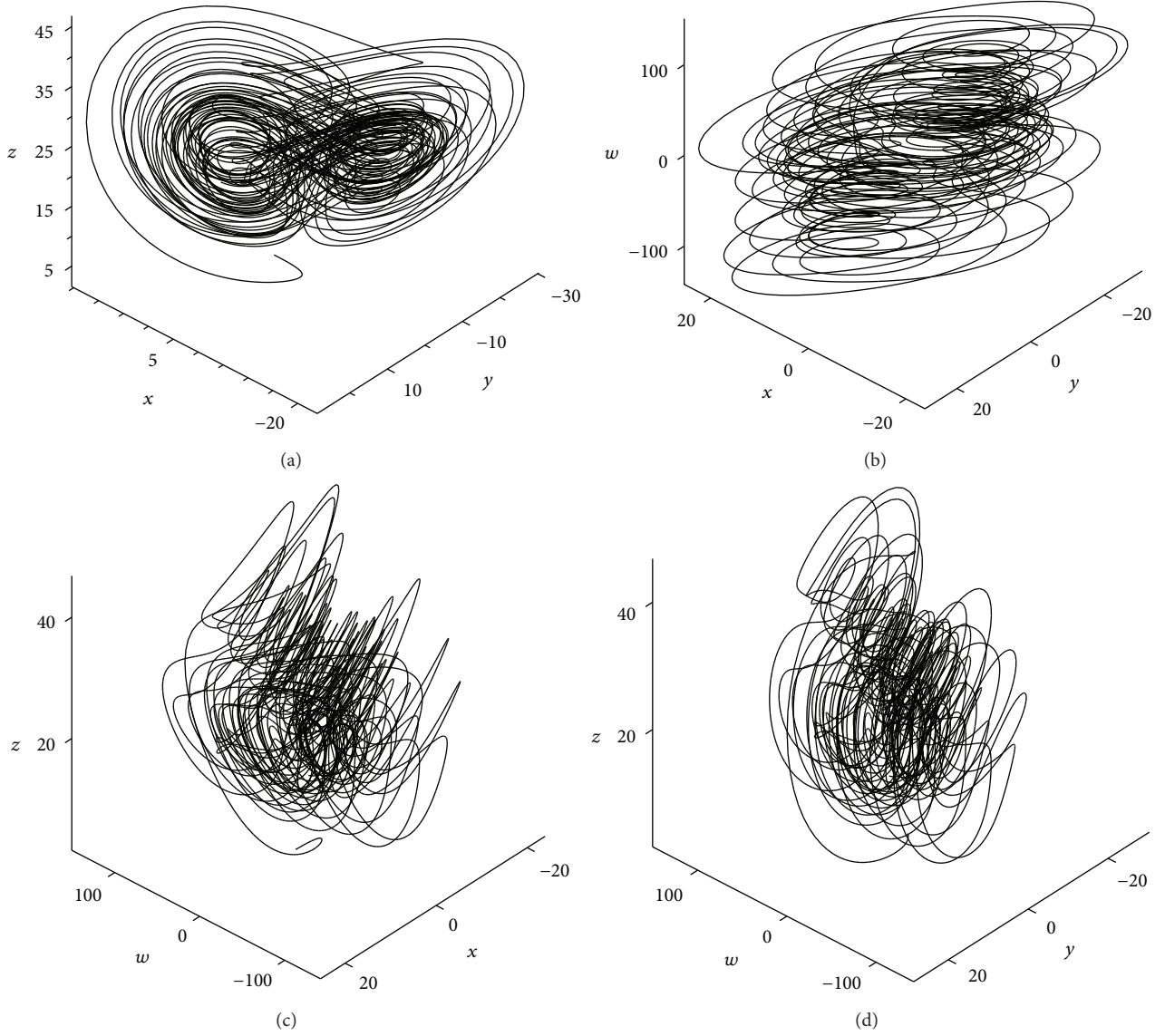


FIGURE 3: Typical dynamical behavior of hyperchaotic Lü system. (a) Projection in (x, y, z) space; (b) projection in (x, y, w) space; (c) projection in (w, x, z) space; (d) projection in (y, z, w) space.

where \hat{a}_j , \hat{b}_j , and \hat{c}_j are the estimates of a_j , b_j , and c_j , respectively, $j = 1, 2$. Choosing the update parameters law as

$$\begin{aligned}
 \dot{\hat{a}}_1 &= -s(y_1 - x_1), \\
 \dot{\hat{b}}_1 &= sx_1, \\
 \dot{\hat{c}}_1 &= -sz_1, \\
 \dot{\hat{a}}_2 &= -s(y_2 - x_2), \\
 \dot{\hat{b}}_2 &= sx_2, \\
 \dot{\hat{c}}_2 &= -sz_2,
 \end{aligned} \tag{27}$$

and applying the control law in (26) to (24) yield the resulting error dynamics as follows:

$$\begin{aligned}
 \dot{e}_1 &= (a_1 - \hat{a}_1)(y_1 - x_1) - (a_2 - \hat{a}_2)(y_2 - x_2), \\
 \dot{e}_2 &= (b_1 - \hat{b}_1)x_1 + (b_2 - \hat{b}_2)x_2 - \frac{6s}{|s| + 0.01}, \\
 \dot{e}_3 &= -(c_1 - \hat{c}_1)z_1 - (c_2 - \hat{c}_2)z_2
 \end{aligned} \tag{28}$$

which is stable by Theorem 1. To show that, we consider the following Lyapunov candidate function:

$$V = \frac{1}{2}s^2 + \frac{1}{2}\|\alpha - \hat{\alpha}\|^2. \tag{29}$$

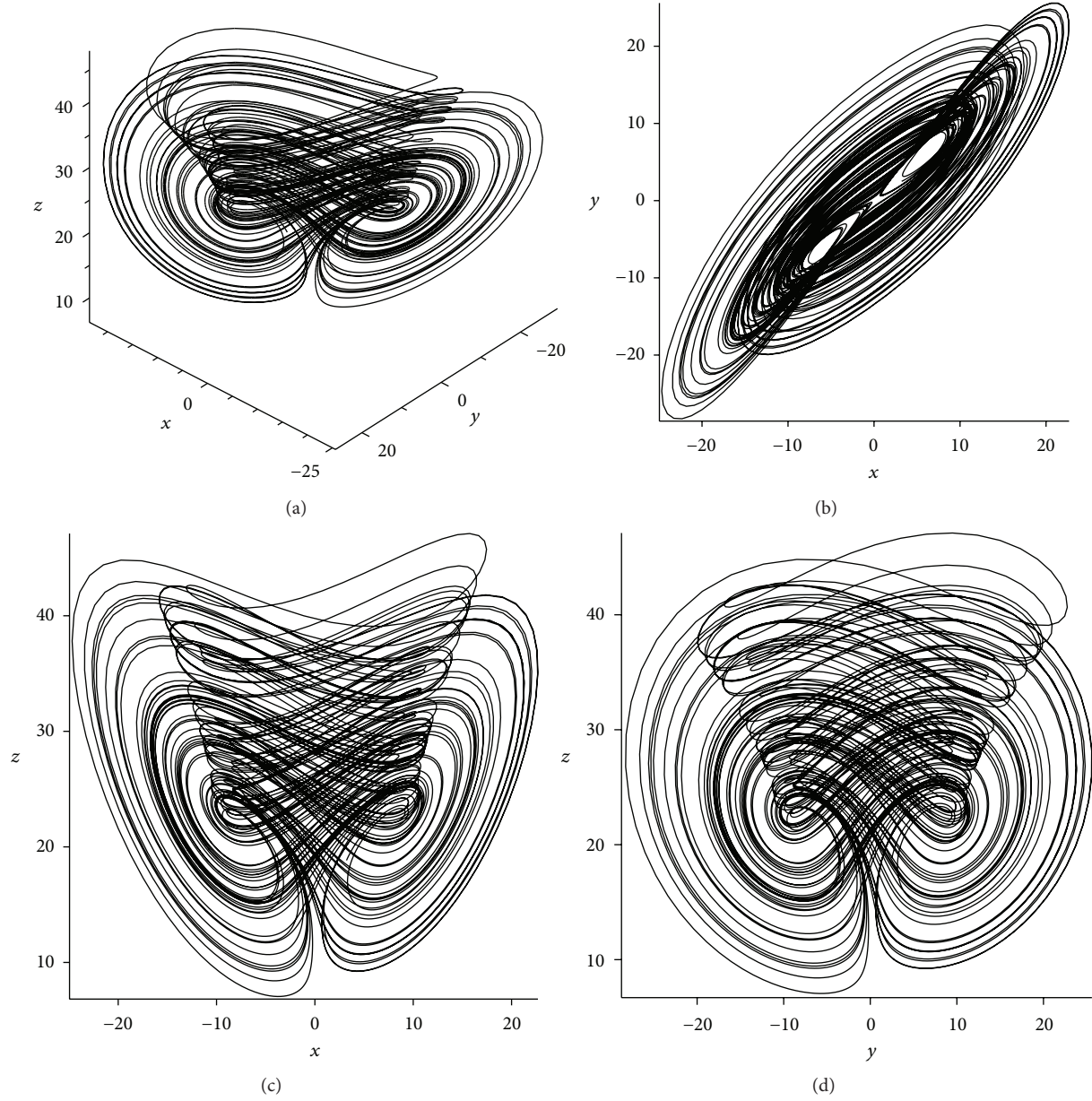


FIGURE 4: Typical dynamical behavior of three-dimensional Chen system. (a) Projection in (x, y, z) space; (b) projection in (x, y) space; (c) projection in (x, z) space; (d) projection in (y, z) space.

The time derivative of (29) is

$$\begin{aligned}\dot{V} &= \dot{s}s - (\alpha - \hat{\alpha})^T \dot{\hat{\alpha}} \\ &= s[\dot{e}_1 + \dot{e}_2 + \dot{e}_3] - \left[(a - \hat{a})\dot{\hat{a}} + (b - \hat{b})\dot{\hat{b}} + (c - \hat{c})\dot{\hat{c}} \right] \\ &= s[a_1(y_1 - x_1) + a_2(y_2 - x_2) \\ &\quad - \hat{a}_1(y_1 - x_1) - \hat{a}_2(y_2 - x_2)] \\ &\quad + s\left[(b_1 - \hat{b}_1)x_1 + (b_2 - \hat{b}_2)x_2 - \frac{6s}{|s| + 0.01}\right] \\ &\quad - s[(c_1 - \hat{c}_1)z_1 - (c_2 - \hat{c}_2)z_2]\end{aligned}$$

$$\begin{aligned}&= -s(a_1 - \hat{a}_1)(y_1 - x_1) + s(b_1 - \hat{b}_1)x_1 \\ &\quad - \frac{6s^2}{|s| + 0.01} - s(c_1 - \hat{c}_1)z_1 \\ &\quad - s(a_2 - \hat{a}_2)(y_2 - x_2) - s(b_2 - \hat{b}_2)x_2 + s(c_2 - \hat{c}_2)z_2.\end{aligned}\tag{30}$$

Then (30) reduces to

$$\dot{V} = -\frac{6s^2}{|s| + 0.01}.\tag{31}$$

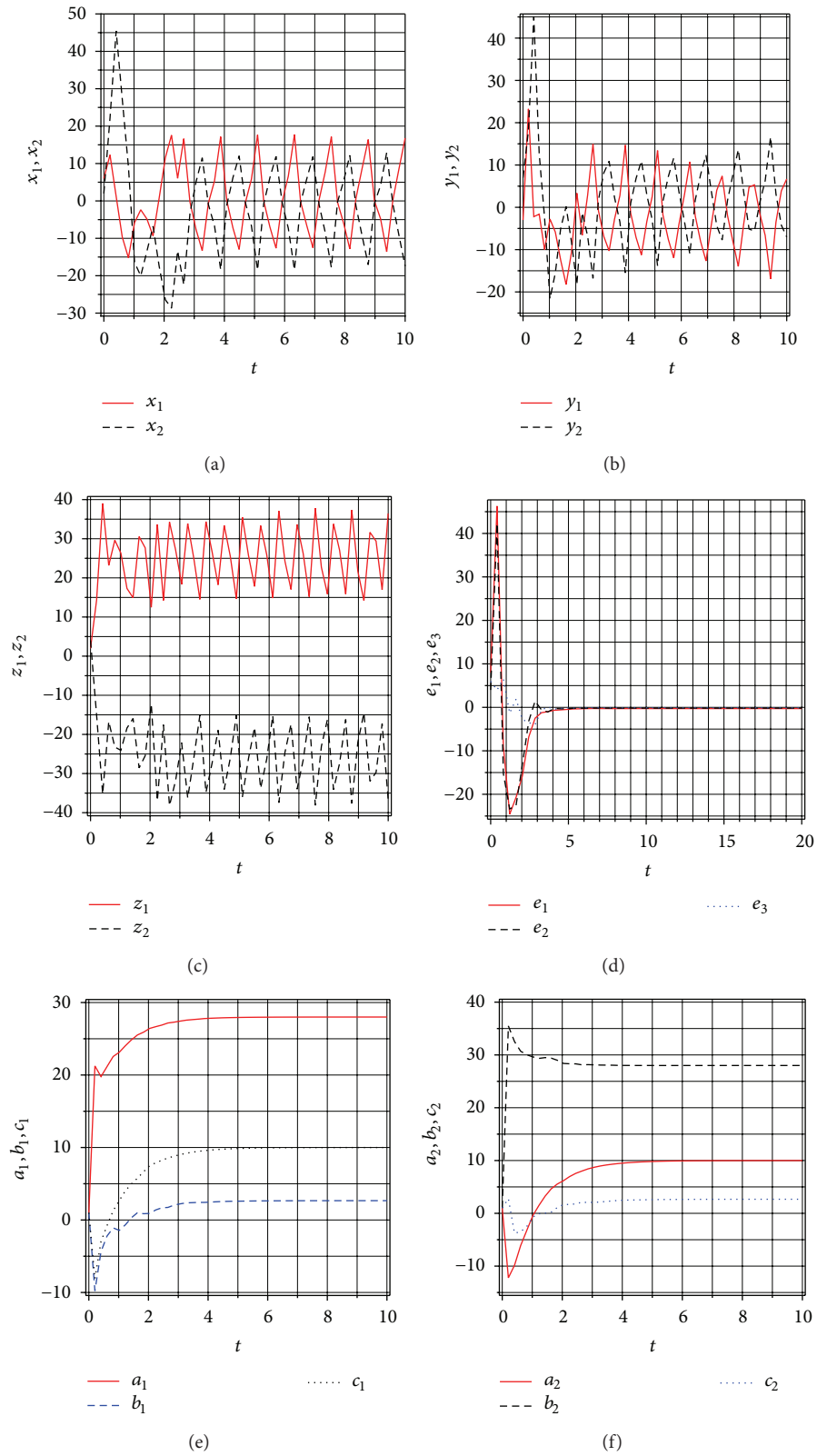


FIGURE 5: State trajectories of drive system (22) and response system (23): (a) signals x_1 and x_2 ; (b) signals y_1 and y_2 ; (c) signals z_1 and z_2 ; (d) the error signals e_1 , e_2 , and e_3 of the hyperchaotic Lorenz and Lorenz systems under the controller (26) and the parameters update law (27); (e)-(f) changing parameters a_1 , b_1 , r_1 and a_2 , b_2 , c_2 of the hyperchaotic Lorenz and Lorenz systems with time t .

Since both $s^2 > 0$ and $|s| > 0$, then we get

$$\dot{V} < 0. \quad (32)$$

Since V is positive definite and \dot{V} is negative definite, then according to Lyapunov Stability Theorem response system (23) can antisynchronize drive system (22) asymptotically. In what follows, we discuss the simulation result for the adaptive sliding mode reduced-order antisynchronization between the hyperchaotic Lorenz system and three-dimensional Lorenz system. In the numerical simulations, the fourth-order Runge-Kutta method is used to solve the systems with time step size 0.0001. For this numerical simulation, we assumed that the initial conditions $(x_1(0), y_1(0), z_1(0), w_1(0)) = (6, -3, 2, 2)$ and $(x_2(0), y_2(0), z_2(0)) = (2, 7, 4)$. Hence the error system has the initial values $e_1(0) = 8$, $e_2(0) = 4$, and $e_3(0) = 6$. The systems parameters are chosen as $a_1 = 10$, $b_1 = 28$, $c_1 = 8/3$, $r_1 = 1.3$, $a_2 = 10$, $b_2 = 28$, and $c_2 = 8/3$ in the simulations such that the first system exhibits hyperchaotic behavior whereas the second one exhibits chaotic behavior. The initial values for the estimated parameters are chosen as $\hat{a}_1(0) = 1$, $\hat{b}_1(0) = 1$, $\hat{c}_1(0) = 1$, $\hat{r}_1(0) = 1$, $\hat{a}_2(0) = 1$, $\hat{b}_2(0) = 1$, $\hat{c}_2(0) = 1$, and $\hat{r}_2(0) = 1$. Reduced-order antisynchronization of the systems (22) and (23) via adaptive sliding mode control law in (26) is shown in Figure 5. Figures 5(a)–5(c) display the state trajectories of drive system (22) and response system (23). Figure 5(d) displays the error signals e_1, e_2 , and e_3 of the systems (22) and (23) under the controller (26). And, the Figures 5(e) and 5(f) show the parameter estimates of the systems (22) and (23), respectively.

5. Adaptive Reduced-Order Sliding Mode Antisynchronization between Hyperchaotic Lü System and Three-Dimensional Chen System

In the manner, similar to the previous example, for the hyperchaotic Lü system, the master system is considered to be the projections in the direction of x , y , and z only. So it can be written as follows:

$$\begin{aligned} \dot{x}_1 &= a_1(y_1 - x_1) + w_1, \\ \dot{y}_1 &= -x_1 z_1 + b_1 y_1, \\ \dot{z}_1 &= x_1 y_1 - c_1 z_1 \end{aligned} \quad (33)$$

and the slave system is considered as the three-dimensional Chen system and can be written as

$$\begin{aligned} \dot{x}_2 &= a_2(y_2 - x_2) + u_1, \\ \dot{y}_2 &= (b_2 - a_2)x_2 - x_2 z_2 + b_2 y_2 + u_2, \\ \dot{z}_2 &= x_2 y_2 - c_2 z_2 + u_3, \end{aligned} \quad (34)$$

where u_1 , u_2 , and u_3 are three control functions to be designed. The error dynamics is represented by

$$\begin{aligned} \dot{e}_1 &= a_1(y_1 - x_1) + a_2(y_2 - x_2) + w_1 + u_1, \\ \dot{e}_2 &= -x_1 z_1 + b_1 y_1 + (b_2 - a_2)x_2 - x_2 z_2 + b_2 y_2 + u_2, \\ \dot{e}_3 &= x_1 y_1 - c_1 z_1 + x_2 y_2 - c_2 z_2 + u_3, \end{aligned} \quad (35)$$

where $e_1 = x_1 + x_2$, $e_2 = y_1 + y_2$, $e_3 = z_1 + z_2$. The control parameters are chosen as $C = (1, 1, 1)$, $K = (1, 1, 0)^T$ and $\gamma = 0.01$. Then the switching surface is equal to

$$\begin{aligned} s(e) &= e_1 + e_2 + e_3, \\ w(t) &= \frac{s}{|s| + 0.01} \end{aligned} \quad (36)$$

and then the adaptive sliding mode control law for the system in (35) is

$$\begin{aligned} u_1 &= -\hat{a}_1(y_1 - x_1) - \hat{a}_2(y_2 - x_2) - w_1 - \frac{s}{|s| + 0.01}, \\ u_2 &= -\hat{b}_1 y_1 - (\hat{b}_2 - \hat{a}_2)x_2 - \hat{b}_2 y_2 + x_1 z_1 \\ &\quad + x_2 z_2 - \frac{s}{|s| + 0.01}, \\ u_3 &= -x_1 y_1 + \hat{c}_1 z_1 - x_2 y_2 + \hat{c}_2 z_2, \end{aligned} \quad (37)$$

where \hat{a}_j , \hat{b}_j , and \hat{c}_j are the estimates of a_j , b_j , and c_j , respectively, $j = 1, 2$. Choosing the update parameters law as

$$\begin{aligned} \dot{\hat{a}}_1 &= s(y_1 - x_1), \\ \dot{\hat{b}}_1 &= s y_1, \\ \dot{\hat{c}}_1 &= -s z_1, \\ \dot{\hat{a}}_2 &= s(y_2 - x_2), \\ \dot{\hat{b}}_2 &= s(x_2 + y_2), \\ \dot{\hat{c}}_2 &= -s z_2 \end{aligned} \quad (38)$$

and applying the control law in (37) to (35) yield the resulting error dynamics as follows:

$$\begin{aligned} \dot{e}_1 &= (a_1 - \hat{a}_1)(y_1 - x_1) + (a_2 - \hat{a}_2)(y_2 - x_2) \\ &\quad - \frac{s}{|s| + 0.01}, \\ \dot{e}_2 &= (b_1 - \hat{b}_1)y_1 + [(b_2 - a_2) - (\hat{b}_2 - \hat{a}_2)]x_2 \\ &\quad + (b_2 - \hat{b}_2)y_2 - \frac{s}{|s| + 0.01}, \\ \dot{e}_3 &= -(c_1 - \hat{c}_1)z_1 - (c_2 - \hat{c}_2)z_2 \end{aligned} \quad (39)$$

which is stable by Theorem 1. To show that, we consider the following Lyapunov candidate function:

$$V = \frac{1}{2}s^2 + \frac{1}{2}\|\alpha - \hat{\alpha}\|^2. \quad (40)$$

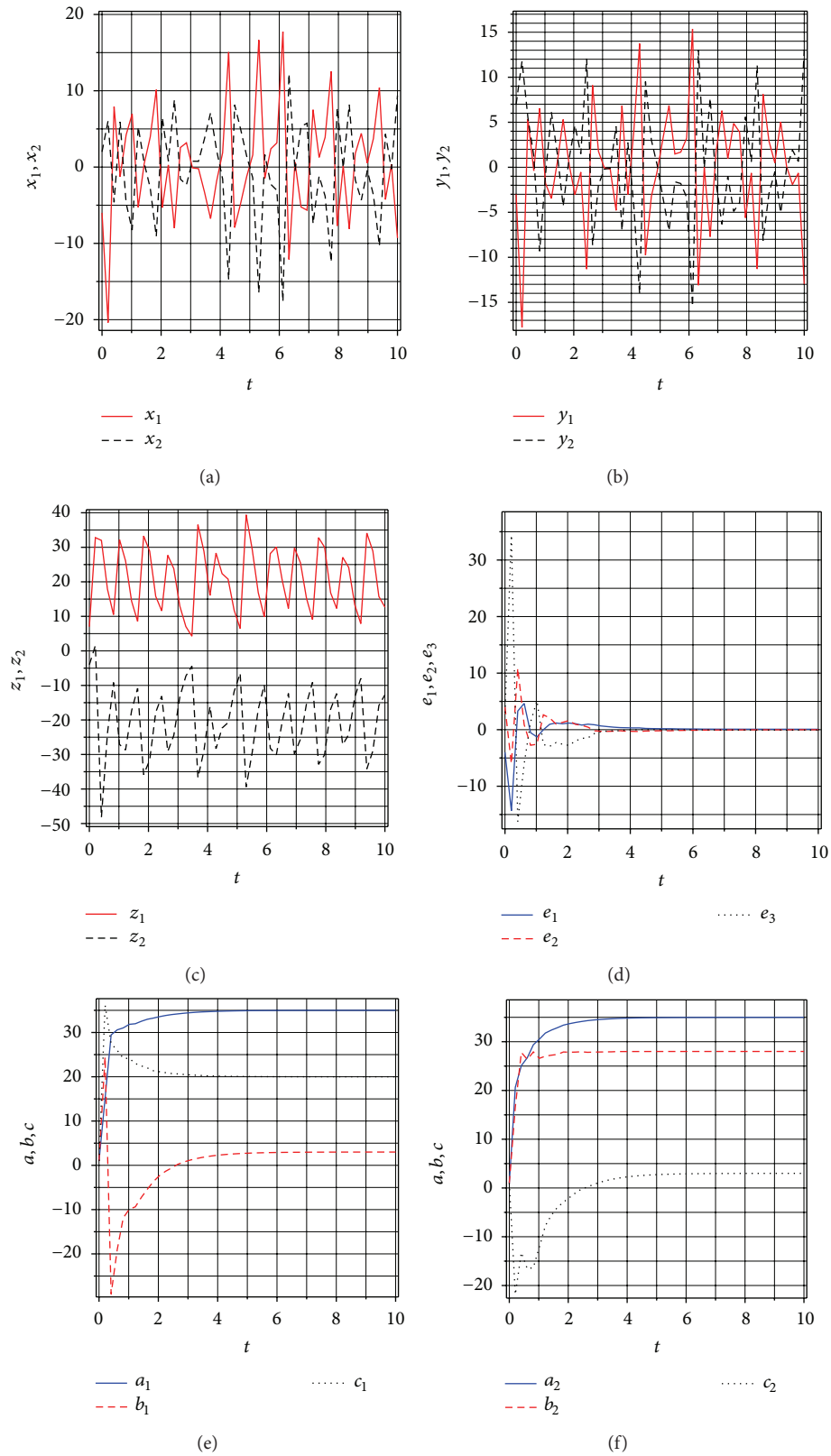


FIGURE 6: State trajectories of drive system (33) and response system (34): (a) signals x_1 and x_2 ; (b) signals y_1 and y_2 ; (c) signals z_1 and z_2 ; (d) the error signals e_1, e_2, e_3 of the hyperchaotic Lü and Chen systems under the controller (37) and the parameters update law (38); (e)-(f) changing parameters a_1, b_1, r_1 and a_2, b_2, c_2 of the hyperchaotic Lü and Chen systems with time t .

The time derivative of (40) is

$$\begin{aligned}
 \dot{V} &= \dot{s}s - (\alpha - \hat{\alpha})^T \dot{\hat{\alpha}} \\
 &= s [\dot{e}_1 + \dot{e}_2 + \dot{e}_3] \\
 &\quad - \left[(a - \hat{a}) \dot{\hat{a}} + (b - \hat{b}) \dot{\hat{b}} + (c - \hat{c}) \dot{\hat{c}} \right] \\
 &= s \left[(a_1 - \hat{a}_1)(y_1 - x_1) + (a_2 - \hat{a}_2)(y_2 - x_2) \right. \\
 &\quad \left. - \frac{s}{|s| + 0.01} \right] \\
 &\quad + s \left[(b_1 - \hat{b}_1)y_1 + [(b_2 - a_2) - (\hat{b}_2 - \hat{a}_2)]x_2 \right. \\
 &\quad \left. + (b_2 - \hat{b}_2)y_2 - \frac{s}{|s| + 0.01} \right] \\
 &\quad - s [(c_1 - \hat{c}_1)z_1 - (c_2 - \hat{c}_2)z_2] \\
 &\quad - s(a_1 - \hat{a}_1)(y_1 - x_1) - s(b_1 - \hat{b}_1)y_1 + s(c_1 - \hat{c}_1)z_1 \\
 &\quad - s(a_2 - \hat{a}_2)(y_2 - x_2) \\
 &\quad - s(b_2 - \hat{b}_2)(x_2 + y_2) + s(c_2 - \hat{c}_2)z_2.
 \end{aligned} \tag{41}$$

Then (41) reduces to

$$\dot{V} = -\frac{2s^2}{|s| + 0.01}. \tag{42}$$

Since both $s^2 > 0$ and $|s| > 0$, then we get

$$\dot{V} < 0. \tag{43}$$

Since V is positive definite and \dot{V} is negative definite, then according to Lyapunov Stability Theorem response system (34) can antisynchronize drive system (33) asymptotically. In what follows, we discuss the simulation result for the adaptive sliding mode reduced-order antisynchronization between the hyperchaotic Lorenz system and three-dimensional Lorenz system. In the numerical simulations, the fourth-order Runge-Kutta method is used to solve the systems with time step size 0.0001. For this numerical simulation, we assumed that the initial conditions $(x_1(0), y_1(0), z_1(0), w_1(0)) = (-6, -3, 7, 2)$ and $(x_2(0), y_2(0), z_2(0)) = (2, 7, 4)$. Hence the error system has the initial values $e_1(0) = -4$, $e_2(0) = 4$, and $e_3(0) = 6$. The system parameters are chosen as $a_1 = 35$, $b_1 = 20$, $c_1 = 3$, $r_1 = -0.4$, $a_2 = 35$, $b_2 = 28$, and $c_2 = 3$ in the simulations such that the first system exhibit's hyperchaotic behavior and the second one exhibits chaotic behavior. The initial values for the estimated parameters are chosen as $\hat{a}_1(0) = 1$, $\hat{b}_1(0) = 1$, $\hat{c}_1(0) = 1$, $\hat{r}_1(0) = 1$, $\hat{a}_2(0) = 1$, $\hat{b}_2(0) = 1$, $\hat{c}_2(0) = 1$, and $\hat{r}_2(0) = 1$. Reduced-order antisynchronization of the systems (33) and (34) via adaptive sliding mode control law in (37) is shown in Figure 6. Figures 6(a)–6(c) display the state trajectories of drive system (33) and response system

(34). Figure 6(d) displays the error signals e_1 , e_2 , and e_3 of the systems (33) and (34) under the controller (37). And, Figures 6(e) and 6(f) show the parameter estimates of the systems (33) and (34), respectively.

6. Concluding Remark

The novelty of our technique in solving reduced-order anti-synchronization problem is demonstrated and proved using rigorous analytical and numerical procedures to antisynchronize two uncertain chaotic systems. The antisynchronization of the dynamical evolution of a 3rd-order chaotic system was realized with the canonical projection of a 4th-order chaotic system even though their parameters were unknown. This was based upon the parameters modulation and the adaptive sliding mode control techniques. The proven techniques were applied to the two examples: Lorenz (4th-order) with Lorenz (3rd-order) and hyperchaotic Lü (4th-order) with Chen (3rd-order). The theoretical analyses and numerical simulations have verified and supported our assumptions. The scope for the applications of antisynchronization of two chaotic systems with different orders is much wide ranging.

Acknowledgment

This work is financially supported by the Universiti Kebangsaan Malaysia Grant: UKM-DLP-2011-016.

References

- [1] A. Alasty and R. Shabani, "Chaotic motions and fractal basin boundaries in spring-pendulum system," *Nonlinear Analysis: Real World Applications*, vol. 7, no. 1, pp. 81–95, 2006.
- [2] M. Chen, D. Zhou, and Y. Shang, "A new observer-based synchronization scheme for private communication," *Chaos, Solitons & Fractals*, vol. 24, no. 4, pp. 1025–1030, 2005.
- [3] O. Diallo and Y. Koné, "Melnikov analysis of chaos in a general epidemiological model," *Nonlinear Analysis: Real World Applications*, vol. 8, no. 1, pp. 20–26, 2007.
- [4] M. Feki, "An adaptive chaos synchronization scheme applied to secure communication," *Chaos, Solitons & Fractals*, vol. 18, no. 1, pp. 141–148, 2003.
- [5] L. M. Pecora and T. L. Carroll, "Synchronization in chaotic systems," *Physical Review Letters*, vol. 64, no. 8, pp. 821–824, 1990.
- [6] D. López-Mancilla and C. Cruz-Hernández, "Output synchronization of chaotic systems under nonvanishing perturbations," *Chaos, Solitons & Fractals*, vol. 37, no. 4, pp. 1172–1186, 2008.
- [7] J.-J. Yan, Y.-S. Yang, T.-Y. Chiang, and C.-Y. Chen, "Robust synchronization of unified chaotic systems via sliding mode control," *Chaos, Solitons & Fractals*, vol. 34, no. 3, pp. 947–954, 2007.
- [8] L. Huang, R. Feng, and M. Wang, "Synchronization of chaotic systems via nonlinear control," *Physics Letters A*, vol. 320, no. 4, pp. 271–275, 2004.
- [9] Q. Zhang and J.-A. Lu, "Chaos synchronization of a new chaotic system via nonlinear control," *Chaos, Solitons & Fractals*, vol. 37, no. 1, pp. 175–179, 2008.

- [10] M. T. Yassen, "On hyperchaos synchronization of a hyperchaotic Lü system," *Nonlinear Analysis: Theory, Methods & Applications*, vol. 68, no. 11, pp. 3592–3600, 2008.
- [11] E. Bai and K. Lonngen, "Synchronization of two Lorenz systems using active control," *Chaos, Solitons & Fractals*, vol. 8, no. 1, pp. 51–58, 1997.
- [12] G.-H. Li and S.-P. Zhou, "Anti-synchronization in different chaotic systems," *Chaos, Solitons & Fractals*, vol. 32, no. 2, pp. 516–520, 2007.
- [13] J. Cao, Z. Wang, and Y. Sun, "Synchronization in an array of linearly stochastically coupled networks with time delays," *Physica A*, vol. 385, no. 2, pp. 718–728, 2007.
- [14] S. Bowong, "Stability analysis for the synchronization of chaotic systems with different order: application to secure communications," *Physics Letters A*, vol. 326, no. 1-2, pp. 102–113, 2004.
- [15] Q. Jia, "Hyperchaos generated from the Lorenz chaotic system and its control," *Physics Letters A*, vol. 366, no. 3, pp. 217–222, 2007.
- [16] E. N. Lorenz, "Deterministic non-periodic flow," *Journal of the Atmospheric Sciences*, vol. 20, no. 2, p. 130, 1963.
- [17] A. Chen, J. Lu, J. Lü, and S. Yu, "Generating hyperchaotic Lü attractor via state feedback control," *Physica A*, vol. 364, pp. 103–110, 2006.
- [18] G. Chen and T. Ueta, "Yet another chaotic attractor," *International Journal of Bifurcation and Chaos*, vol. 9, no. 7, pp. 1465–1466, 1999.